Available online at www.sciencedirect.com
SCIENCE DIRECT®
Journal of Chromatography A, 1079 (2005) 173–186
JOURNAL OF CHROMATOGRAPHY A
www.elsevier.com/locate/chroma

Binding behaviour and conformational properties of globular proteins in the presence of immobilised non-polar ligands used in reversed-phase liquid chromatography

Reinhard I. Boysen, Agnes J.O. Jong, Milton T.W. Hearn *

Australian Research Council Special Research Centre for Green Chemistry, Australian Centre for Research on Separation Science, Monash University, Clayton, Vic. 3800, Australia

Available online 18 April 2005

This manuscript is dedicated to the memory of Csaba Horváth, a friend, mentor, scientific innovator and a beacon of inspiration for this laboratory for more than 30 years.

Abstract

The thermodynamic and extra-thermodynamic dependencies of five types of cytochrome *c* in water–acetonitrile mixtures of different composition in the presence of immobilised *n*-octyl ligands as a function of temperature from 278 K to 338 K have been investigated. The corresponding enthalpic, entropic and heat capacity parameters, $\Delta H^{\circ}_{\text{assoc}}$, $\Delta S^{\circ}_{\text{assoc}}$ and ΔC°_{p}, have been evaluated from the observed non-linear Van't Hoff plots of these globular proteins in these heterogeneous systems. The relationships between the free energy dependencies, various molecular parameters and extra-thermodynamic dependencies (empirical correlations) of these protein–non-polar ligand interactions have also been examined. Thus, the involvement of enthalpy-entropy compensation effects has been documented for the binding of these cytochrome *c*s to solvated *n*-octyl ligands. Moreover, the results confirm that this experimental approach permits changes in molecular surface area due to the unfolding of these proteins on association with non-polar ligands as a function of temperature to be correlated with other biophysical properties. This study thus provides a general procedure whereby the corresponding free energy dependencies of globular proteins on association with solvated non-polar ligands in heterogeneous two-phase systems can be quantitatively evaluated in terms of fundamental molecular parameters.
© 2005 Published by Elsevier B.V.

Keywords: Cytochrome *c*; Van't Hoff plots; Free energy relationships; Molecular parameters; Entropy–enthalpy compensation; Surface area dependencies; Amino acid substitution; Reversed-phase chromatography

1. Introduction

Elucidation and quantitation of the molecular and atomic processes that control the folding and/or unfolding of proteins in bulk solution and at liquid/solid or liquid/liquid interfaces currently represents an area of intense research interest. Arising from these studies, a variety of paradoxical situations have been documented when globular proteins are exposed to organic solvents or other substances, particularly if a non-polar sorbent surface is also involved. For example, many globular proteins can be purified in their bioactive state at laboratory scale under one set of reversed-phase liquid chromatographic (RPC) or hydrophobic interaction chromatographic (HIC) conditions, yet under another set of conditions, which differ only slightly in terms of temperature or the concentration of an organic solvent or salt, the same proteins are denatured [1–3]. Addition of an organic solvent, such as acetonitrile or methanol, to an aqueous solution is known to reduce the surface tension of the mixture, leading to a lower temperature at which denaturation of a protein can occur. Other studies have shown [4,5] that at relatively high concentrations of acetonitrile or some other solvents they can act as denaturants for many globular proteins at higher temperatures, yet the ther-

* Corresponding author. Tel.: +61 3 9905 4547; fax: +61 3 9905 8501.
E-mail address: milton.hearn@sci.monash.edu.au (M.T.W. Hearn).

0021-9673/$ – see front matter © 2005 Published by Elsevier B.V.
doi:10.1016/j.chroma.2005.03.097

modynamic stability of the same proteins can be increased over a defined temperature range by lower concentrations of these solvents.

With bulk water–organic solvent systems, changes in the thermodynamic parameters associated with protein–ligand interactions or protein unfolding/refolding processes are typically described in terms of the Gibbs–Helmholtz equation, such that the change in the free energy of association, $\Delta G^{\circ}_{\text{assoc}}$ or the change in the free energy of unfolding (denaturation), $\Delta G^{\circ}_{\text{unfold}}$, as a function of the temperature, T (in K), can be expressed by Eqs. (1) and (2) respectively:

$$\Delta G^{\circ}_{\text{assoc}} = \Delta H^{\circ}_{\text{assoc}} - T\Delta S^{\circ}_{\text{assoc}} \quad (1)$$

$$\Delta G^{\circ}_{\text{unfold}} = \Delta H^{\circ}_{\text{unfold}} - T\Delta S^{\circ}_{\text{unfold}} \quad (2)$$

In the case of reversible, equilibrium protein–ligand interactions, evaluation of $\Delta G^{\circ}_{\text{assoc}}$ permits the change in enthalpy of association and change in entropy of association, $\Delta H^{\circ}_{\text{assoc}}$ and $\Delta S^{\circ}_{\text{assoc}}$ respectively, to be determined, whilst for the protein unfolding case measurement of $\Delta G^{\circ}_{\text{unfold}}$ permits the corresponding enthalpic ($\Delta H^{\circ}_{\text{unfold}}$) and entropic ($\Delta S^{\circ}_{\text{unfold}}$) terms to be quantified. For a solution of fixed composition and pH, the binding of a protein to a specific ligand under 'near-equilibrium' conditions can be expressed in terms of the dependency of the concentrations of the protein in the bound and free state, such that the relationship between the equilibrium association constant, K_{assoc}, and $\Delta G^{\circ}_{\text{assoc}}$ is given by:

$$K_{\text{assoc}}\frac{[P]_{\text{bound}}}{[P]_{\text{free}}} = \mathrm{e}^{-\Delta G^{\circ}_{\text{assoc}}/RT} \quad (3)$$

Corresponding expressions can be employed to describe the unfolding of a protein in bulk solution or when bound to immobilised ligands, such that

$$K_{\text{unfold}} = \frac{[P]_{\text{unfold}}}{[P]_{\text{native}}} = \mathrm{e}^{-\Delta G^{\circ}_{\text{unfold}}/RT} \quad (4)$$

Previously, the thermodynamic properties of many globular proteins in association with the surrounding solvent or with free and/or immobilised ligands have often been assumed to be invariant with respect to the temperature, T, of the system. As a consequence, the contributions from the corresponding changes in enthalpy ($\Delta H^{\circ}_{\text{assoc}}$ or $\Delta H^{\circ}_{\text{unfold}}$) and entropy ($\Delta S^{\circ}_{\text{assoc}}$ or $\Delta S^{\circ}_{\text{unfold}}$) to the overall Gibbs free energy change associated with the protein–ligand interaction or protein unfolding have also been considered to be independent of T. In such cases, the change in the heat capacity of the system, ΔC°_{p}, will also be temperature-independent. Based on these considerations, data obtained under one set of solvent- and temperature-conditions have been extrapolated in order to predict experimental conditions that could be more favourable for the stabilisation of the protein of interest in solution or to maximise the association free energy change for interaction of the protein with a specific ligand in the free or immobilised state at a liquid/solid interface. Experimentally, the observation has, however, often been made that the ranges of temperature and solvent compositions over which these stabilisation changes occur or protein–ligand association binding constants reach maximal values cannot be predicted with any accuracy from such empirical procedures.

By convention, when immobilised ligands (syn. ligates) are present as part of a heterogeneous liquid-solid system of defined solvent composition, temperature, pH and phase ratio, Φ, ($=V_{\text{S}}/V_{\text{M}}$, where V_{S} and V_{M} are the volume of the immobilised ligands on an inert solid support material and the volume of the bulk liquid in the system, respectively), then the equilibrium association constant, K_{assoc}, for the protein–ligand interaction can be evaluated [6] from knowledge of the number of moles of the protein that exists in the bound (n_{S}) and free (n_{M}) states and the unitless binding variable (also known in a chromatographic context as the retention factor) k ($=[(n_{\text{S}}/n_{\text{M}}) \times \Phi]$) such that:

$$\ln K_{\text{assoc}} = \ln k - \ln \Phi = -\frac{\Delta G_{\text{assoc}}}{RT} \quad (5)$$

Under isothermic binding conditions, plots of $\ln k$ versus $1/T$ for the interaction of low molecular weight pharmaceutical compounds and amino acids with immobilised non-polar ligands take the form of the well known linear Van't Hoff dependency with the $\Delta H^{\circ}_{\text{assoc}}$ and $\Delta S^{\circ}_{\text{assoc}}$ values determined by linear regression analysis from the respective slope and intercept values. Data derived from several studies [2,7,8] have demonstrated that changes in Φ at specified solvent compositions are usually small (i.e. $\leq\pm$10%) over the examined T range when n-alkylsilicas are used, suggesting that the contribution of $\ln \Phi$ term to the $\ln k$ values is small and essentially constant. These studies have also indicated that the partial molar volumes, υ_{p}, of peptides and proteins only vary to a very small extent (i.e. <5%) in the pressure range of ~220–250 bar and even smaller changes in υ_{p} were predicted to occur for small organic molecules. However, in an increasing number of investigations with polypeptides and proteins when bound to non-polar ligands in batch adsorption studies or when separated under high-performance RPC or HIC conditions, significant divergences from this ideal behaviour have been found with the corresponding Van't Hoff behaviour exhibiting non-linear dependencies on T and solvent composition with the corresponding enthalpic, $\Delta H^{\circ}_{\text{assoc}}$, entropic, $\Delta S^{\circ}_{\text{assoc}}$, and heat capacity, ΔC°_{p}, terms all showing strong temperature dependencies [2,5,7,8]. In order to provide a more quantitative description of the effect of co-solvents or T on the stability of globular proteins in the presence of non-polar ligands, we have utilized in this investigation a recently developed experimental approach [7] to quantitatively assess the magnitude of the changes in several molecular properties, including the accessible surface area, when equine cytochrome c unfolds due to variations in the temperature of the surrounding solvent and associated micro-environment. In particular, this approach has permitted the thermodynamic changes associated with the unfolding of this and several homologous proteins to be determined in the presence of immobilised n-octyl ligands over the temperature range 278–338 K. Moreover, these

studies with cytochrome *c* homologues have permitted the impact of individual amino acid substitutions on the respective free energy and extra-thermodynamic dependencies to be evaluated. These investigations have thus validated a general experimental procedure for the quantitative assessment of the temperature-dependent behaviour of families of globular or non-globular proteins on association with non-polar ligands as the composition of the surrounding solvent is adjusted.

2. Experimental

Acetonitrile (ACN) and methanol (HPLC grade) were obtained from Biolab Scientific (Melbourne, Australia) and trifluoroacetic acid (TFA) from Auspep (Melbourne, Australia). Water was double distilled and deionized using a Milli-Q system (Millipore, Bedford, MA, USA). The cytochrome *c*s from different species (*Bos Taurus* (bovine), *Canis lupus familiaris* (canine), *Gallus gallus* (chicken), *Equus caballus* (equine), and *Thunnus alalunga* (tuna) were obtained from Sigma (St. Louis, MO, USA) and were characterised by electrospray ionization (ESI) MS, capillary zone electrophoresis (CZE) and sodium dodecyl sulfate-polyacrylamide gel electrophoresis (SDS-PAGE) prior to use. Bulk solvent mixtures of different compositions were filtered and degassed by sparging with nitrogen. All *k* determinations were performed with a HP 1090/HP Chemstation instrument (Hewlett-Packard, USA) using 150 × 4.6 mm I.D. columns packed with 5 μm particle sized Zorbax 300 SB-C8 non-polar sorbent obtained from Rockland Technologies, (Littlefalls, DE, USA) operated at a flow rate of 1 ml/min. The experimental data were acquired using different acetonitrile–water mixtures containing between 30 and 34% (v/v) acetonitrile and 0.09% (v/v) TFA and methanol–water mixtures containing between 60 and 65% (v/v) methanol and 0.09% (v/v) TFA at temperatures between 278 and 335 K in 5 K increments. The temperature was controlled by immersing the column in a thermostated coolant-jacket coupled to a recirculating cooler (Colora Messtechnik, Lorch/Wutt, Germany). The *k* values were calculated for a standard set of operating conditions based on methods described elsewhere [6] The total volume, V_T, the stationary phase volume, V_S, the free solvent phase volume, V_M, and the phase ratio, Φ, of the system using the non-interactive solute, sodium nitrate. All retention factor values (*k*) were derived at least from duplicate measurements with the standard error of the mean (SEM) for replicates typically varying by less than 1%. In all figures presented, the SEMs of the replicate measurements were smaller than the symbols used for the data points. Protein solutions were prepared at a concentration of 1 mg/ml in 0.09% (v/v) TFA in water. All measurements were carried out under experimental conditions favouring protein adsorption to the Zorbax 300 SB-C8 non-polar sorbent within a linear region of the adsorption isotherm, i.e. involved between 2 and 8 μg protein per g sorbent in each experiment. Various experimental and thermodynamic parameters were calculated using the *Eudoxos* and *Hephaestus* software developed in this laboratory, coupled to the Microsoft Excel 5.0 program whilst the statistical analysis involved the Jandel Scientific Sigma plot 4.01 linear and non-linear regression analysis.

Molecular modelling studies were carried out using the CS Chem3D Pro 4.0 software (CambridgeSoft, Cambridge, MA, USA). The molecular surface area, ΔA_{mol}, solvent accessible surface area, ΔA_{solv}, and hydrophobic surface area, ΔA_{hydr}, of the cytochrome *c*s in their folded (globular) conformation were calculated according to the procedures of Eisenhaber and Argos [9] from X-ray crystallographic and homology modelling data, whilst the corresponding surface areas for the cytochrome *c*s in their unfolded conformation were calculated according to the procedures described by Creighton [10], based on the average hydrodynamic properties of these proteins [11] using the procedures of [12]. Hydrophobic moments were calculated according to the methods of Eisenberg and coworkers [13]. The molecular masses of the purified cytochrome *c*s were determined by ESI-MS using a Micromass platform (II) quadrupole MS with an electrospray source with Masslynx NT Ver. 3.2 software (Micromass, Cheshire, UK). The proteins in 1:1 (v/v) acetonitrile–water containing with 3% (v/v) formic acid were infused into the instrument at a speed of 10 μl/min. The ESI-MS spectra of the cytochrome *c*s were acquired at 70 °C at 55 V/50 V over the mass/charge (*m*/*z*) range of 200–2000. Circular dichroism (CD) spectra in the far UV (200–250 nm) of the cytochrome *c*s were recorded on a JASCO J-810 spectropolarimeter (Tokyo, Japan). Spectra were obtained for samples containing 842 μM and 1516 μM of each protein in 10 mM phosphate buffer (pH 7), 30% (v/v) acetonitrile aquo-organic solvent and 63% methanol aquo-organic solvent. CD spectroscopy measurements were performed using a quartz cell with a path length of 2 mm. The spectra were recorded with a bandwidth of 1 nm and scanning rate of 10 nm/min. The resolution for the spectra (data pitch) was 0.1 nm/min. Acquisition of the final spectrum was an average of 5 scans and corrected for backgrounds readings. Wavelength scans of the spectra were studied in 10 K intervals from 283 K to 333 K with the temperature controlled by a Peltier unit. Secondary structure calculations were performed according to the procedures described previously [14,15].

3. Results and discussion

As part of our recent investigations [7,8,16], the thermodynamic and extra-thermodynamic basis of the non-linear Van't Hoff behaviour of several small polypeptides in association with non-polar ligands has been examined in different experimental systems. The present study extends these earlier observations and provides a general framework to evaluate changes in the respective thermodynamic parameters that arise when globular proteins unfold in hydrophobic environments as the temperature is varied. This approach has also enabled the relationship between these thermodynamic param-

eters and structural properties, such as the molecular contact area established between the protein and the ligand(s), to be quantitatively assessed. In particular, as part of this study the changes in the interactive behaviour of several cytochrome *c*s with immobilised *n*-octyl ligands were determined from the changes in the corresponding the logarithmic retention factor k ($\ln k$) values as the composition of acetonitrile/water or methanol/water mixtures was varied over a narrow incremental range with the temperature increased from 278 K to 338 K in 5 K increments.

3.1. Protein ligand interaction in acetonitrile–water mixtures

The Van't Hoff plots ($\ln k$ versus $1/T$) for the various cytochrome *c* species determined with these slightly different acetonitrile–water compositions are shown in Fig. 1A–E. Under the standard operating conditions employed [6], the comparative variations in the shape of the Van't Hoff plots for a series of homologous proteins reflect differences in protein–ligand interactions that have their origin in the nature and extent of change in surface-exposure of the hydrophobic and polar amino acid residues of the proteins. As evident from the results shown in Fig. 1A–E, although the shapes of the Van't Hoff plots overall are similar, there are nevertheless noticeable shifts to increased $\ln k$ values, and thus to larger equilibrium binding constants, K_{assoc}, and greater changes in the Gibbs free energy of association, ΔG°_{assoc}, from equine cytochrome *c* to tuna or bovine cytochrome *c*, then to canine and finally to chicken cytochrome *c* for all φ values at a defined temperature. The Van't Hoff plots for all cytochrome *c* species in different solvent compositions could be fitted to a quadratic relationship, with correlation coefficients r^2 between 0.9842 and 0.9994 at a 95% confidence level, i.e. for canine cytochrome *c* in Fig. 1A.

Moreover, in all cases, non-linear dependencies of $\ln k$ on $1/T$ for these cytochrome *c* species were observed, reflecting the heterothermic nature [2,7] of the protein–ligand interaction, i.e. a process whereby $\Delta C^{\circ}_{p} \neq 0$ and dependent on T. Similarly, the variations in ΔG°_{assoc} for the protein–non-polar ligand association as a function of T were also non-linear, cf. the dependency of $\ln k$ on ΔG°_{assoc} (Eqs. (3)–(5)). As a consequence of recent developments in the characterisation of such heterothermic processes [7], it is possible to derive the corresponding ΔH°_{assoc}, ΔS°_{assoc} and ΔC°_{p} values for different T and cosolvent compositions using the *Hephaestus* software program. Plots of ΔH°_{assoc} versus T (Fig. 2A–E), ΔS°_{assoc} versus T (data not shown) and ΔC°_{p} versus T (Fig. 3A–E) were thus generated for all cytochrome *c* species. As shown in Fig. 2A–E and Fig. 3A–E, the dependencies between ΔH°_{assoc}, ΔS°_{assoc} (data not shown) or ΔC°_{p} on T at different

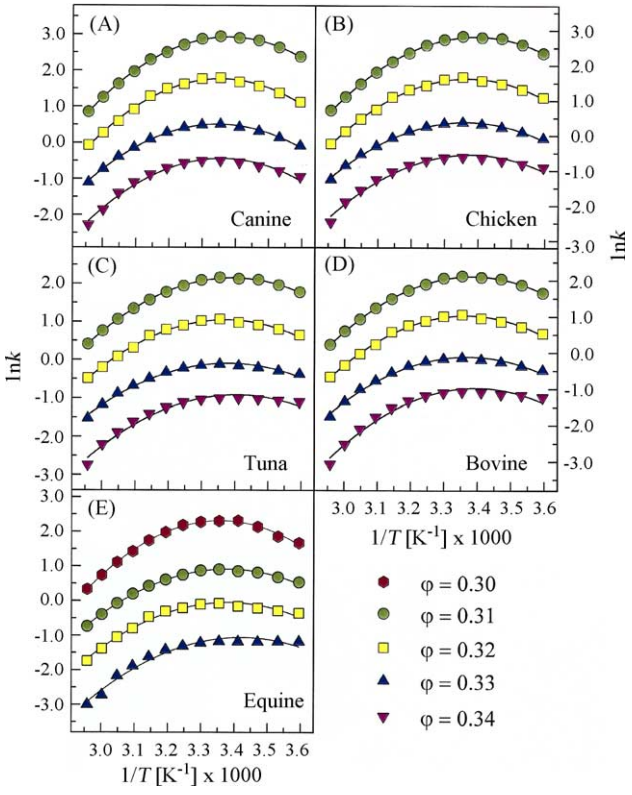

Fig. 1. Van't Hoff plots of the logarithmic binding variable $\ln k$ vs. $1/T$ for canine (A), chicken (B), tuna (C), bovine (D) and equine (E) cytochrome *c* at different volume fractions, φ, of acetonitrile in the water–organic solvent mixture.

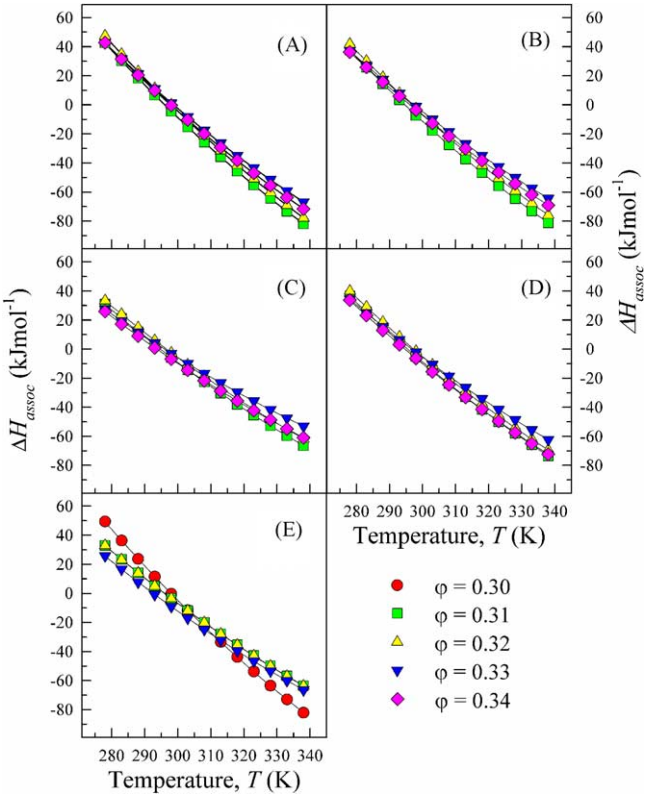

Fig. 2. Plots of the change in enthalpy, ΔH°_{assoc}, vs. T for canine (A), chicken (B), tuna (C), bovine (D) and equine (E) cytochrome *c* at different volume fractions, φ, of acetonitrile in the water–organic solvent mixture.

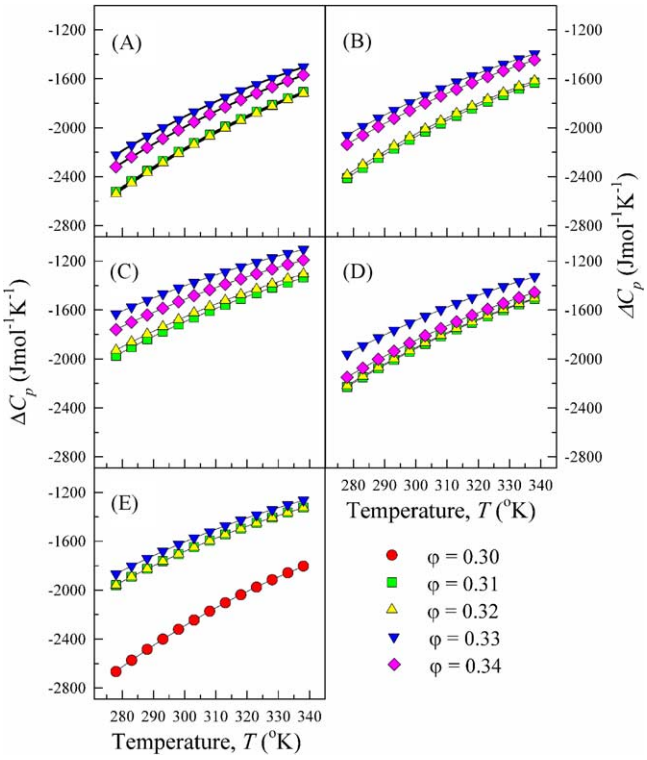

Fig. 3. Plots of the change in heat capacity, ΔC_p°, vs. T for canine (A), chicken (B), tuna (C), bovine (D) and equine (E) cytochrome *c* at different volume fractions, φ, of acetonitrile in the water–organic solvent mixture.

φ-values were essentially linear. Since the slopes of the plots of ΔH_{assoc}° versus T are statistically indistinguishable, this finding indicates that ΔC_p° is independent of the acetonitrile concentration over the range of solvent compositions investigated. However, the plots of ΔH_{assoc}° and ΔG_{assoc}° versus the volume fraction, φ, of acetonitrile at specific temperatures were non-linear (data not shown). From the results shown in Fig. 2A–E and from the plots of the ΔH_{assoc}° versus volume fraction, φ, the conclusion can be drawn that as the concentration of acetonitrile increases, ΔH_{assoc}° reaches a maximum value for each cytochrome *c*. The increase in the value of ΔH_{assoc}° up to a specific φ-value at a particular T value is consistent with the findings of Murphy [17] whereby diminution of the hydrophobic contribution to the association enthalpy rather than a significant change in the hydrogen bonding contribution results in the observed changes in ΔH_{assoc}°. Moreover, as evident from the plots of ΔG_{assoc}° versus the volume fraction, φ, the influence of acetonitrile as a stabilising cosolvent decreases as the volume fraction increases. This finding is in accord with the known solution properties of acetonitrile, whereby this solvent at lower concentrations prefers to form cosolvent clusters with itself due to dipole–dipole interactions and charge repulsion effects rather than disrupting the hydrogen bonding or salt-bridging patterns of proteins [2,8,18–20]. The thermodynamic behaviour exhibited by these cytochrome *c*s is, however, substantially different to that found for some other polypeptides or proteins in the presence of non-polar ligands, such as insulin or mutants related to the transcription factors c-*fos*/c-*jun*, where non-linear dependencies of ΔH_{assoc}°, ΔS_{assoc}° or ΔC_p° on T have also been observed [21]. As expected from the similarity in molecular structures of the different cytochrome *c* species, the changes in ΔH_{assoc}° (Fig. 2A–E), ΔS_{assoc}° (data not shown) or ΔC_p° (Fig. 3A–E) at different φ-values were relatively small. From these results the conclusion can be drawn that all of the cytochrome *c*s adopt similar, relatively compact and stabilised globular structures in these solvent combinations under the different temperature conditions, a finding consistent with results from circular dichroism investigations, as discussed below.

3.2. The entropy–enthalpy compensation of the protein–non-polar ligand interaction in acetonitrile–water mixtures

As represented by the Gibbs–Helmholtz equation, Eq. (1), the change in Gibbs free energy for a protein–ligand interaction involves two often compensating components, the entropy change, ΔS_{assoc}° and the enthalpy change, ΔH_{assoc}°. A negative Gibbs free energy indicates a favourable interaction between ligand and protein [22]. Fig. 4 show the plot of ΔS_{assoc}° versus ΔH_{assoc}° for all cytochrome *c* species at an acetonitrile–water composition of $\varphi = 0.31$. The linearity of these plots confirms that the adsorption behaviour

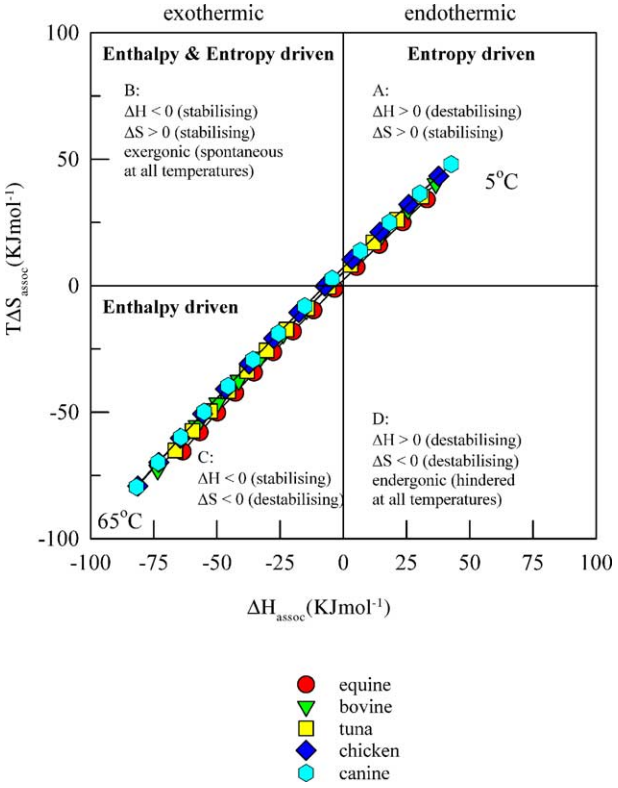

Fig. 4. Entropy ($T\Delta S_{assoc}^\circ$)–enthalpy (ΔH_{assoc}°) compensation plot for canine, chicken, tuna, bovine and equine cytochrome *c* at a φ-value of 0.31.

of these cytochrome *c*s on binding to these hydrophobic ligands is associated with entropy–enthalpy compensation. Compensation of entropy and enthalpy is a characteristic of any interactive system comprising multiple, weak, intermolecular forces [23]. Entropy–enthalpy compensation is not a universal or thermodynamically necessary criterion for protein interaction with non-polar ligands, but rather is determined by a particular pattern of molecular interactions [24]. The binding of a globular protein such as equine cytochrome *c* to immobilised ligands in any molecular system (including solvent) will be exothermic (i.e. $\Delta H^{\circ}_{\text{assoc}} < 0$, cf. Fig. 2), but will be compensated by a decrease in entropy resulting from a reduced degree of molecular flexibility.

As evident from the $\Delta G^{\circ}_{\text{assoc}}$ versus the volume fraction, φ, dependencies (data not shown), for the majority of the experimental conditions a thermodynamically favourable binding process occurs between the various cytochrome *c*s and the non-polar ligands. However, in the regime where sterimolar/hydrodynamic effects can make a more significant contribution to the process, i.e. within the range of *k* values between 0 and 1, small, positive $\Delta G^{\circ}_{\text{assoc}}$ values are obtained. In this region of the experimental conditions, more extensive unfolding of the cytochrome *c*s may occur in the bulk solvent, leading to less favourable interactions between the protein and the immobilised non-polar ligand. Due to the large negative ΔC°_{p}, the enthalpy and entropy functions are strongly temperature dependent. From the experimental data obtained in the present study, it is apparent that the entropy–enthalpy compensation is confined to the temperature range between T_{COLD} and T_{HOT}. Above the hot compensation temperature, T_{HOT}, the dominant term contributing to the Gibbs energy balance is the entropy. Here, the gain of conformational freedom, caused by raising $T > T_{\text{HOT}}$ is not compensated by a corresponding enthalpy change. Below the cold compensation temperature, T_{COLD}, the dominant term is the enthalpy contribution. In this case, the interaction of the protein with the solvent destabilises the protein–ligand interaction, whereby from an energetic point of view, the protein prefers to associate with the solvent rather than with the ligand, mainly through the interaction of the polypeptide backbone (CONH groups) with the water in the eluent, despite the greater potential to undergo unfolding processes. The significance of entropy–enthalpy compensation in protein–ligand interactions lies in its contribution to protein stabilisation in vitro and in vivo in such a way that changes in the environment result in an ability to tolerate large changes of $\Delta H^{\circ}_{\text{assoc}}$ and $\Delta S^{\circ}_{\text{assoc}}$ but are reflected in relatively small effects on $\Delta G^{\circ}_{\text{assoc}}$ [22]. For horse cytochrome *c* at $\varphi = 0.30$ (data not shown) the enthalpy ($\Delta H^{\circ}_{\text{assoc}}$) versus *T* plots and entropy ($T\Delta S^{\circ}_{\text{assoc}}$) versus *T* plots are non-linear and intersect at two points just outside the measured temperature range corresponding to the cold and hot compensation points, $T_{\text{COLD}} = 261.45$ K (−11.7 °C) and $T_{\text{HOT}} = 340.78$ K (67.6 °C). Below T_{COLD} and above T_{HOT} the value for $\Delta G^{\circ}_{\text{assoc}}$ become positive, indicating an unfavourable protein–ligand interaction. In this particular case these values have associated a large error, since they were derived through extrapolation. However, in many other cases, they are well inside the measured temperature range. Nevertheless, they define, in a more qualitative sense, the temperature range of entropy–enthalpy compensation.

Fig. 4 can be divided into four regions, namely A, B, C and D, by drawing vertical lines to mark another kind of compensation temperatures, T_{S} ($T_{\text{S}}\Delta S^{\circ}_{\text{assoc}} = 0$) and ($T_{\text{H}}(\Delta H^{\circ}_{\text{assoc}} = 0)$). In region A, $\Delta H^{\circ}_{\text{assoc}} > 0$ (i.e. the enthalpy change is destabilizing in terms of the protein–ligand interaction) and $\Delta S^{\circ}_{\text{assoc}} > 0$ (i.e. the entropy change is stabilizing in terms of the protein–ligand interaction). In region B, $\Delta H^{\circ}_{\text{assoc}} < 0$ and $\Delta S^{\circ}_{\text{assoc}} > 0$ (both stabilizing in terms of the protein–ligand interaction). In region C, $\Delta H^{\circ}_{\text{assoc}} < 0$ (stabilizing in terms of the protein–ligand interaction) and $\Delta S^{\circ}_{\text{assoc}} < 0$ (destabilizing in terms of the protein–ligand interaction). Finally, in region D, $\Delta H^{\circ}_{\text{assoc}} > 0$ (i.e. the enthalpy change is destabilizing in terms of the protein–ligand interaction) and $\Delta S^{\circ}_{\text{assoc}} < 0$ (destabilizing in terms of the protein–ligand interaction). Characteristic of each of the plots are the corresponding compensation temperatures, which can be calculated from the following formulas, or alternatively, determined graphically:

$$T = \frac{2\text{Rb}_{(2)}}{\Delta H^{\circ}_{\text{assoc}} - \text{Rb}_{(1)}} \qquad \text{for } \Delta H^{\circ}_{\text{assoc}} = 0, \quad T = T_{\text{H}} \tag{6}$$

$$T = \sqrt{\frac{-\text{Rb}_{(2)}}{\Delta S^{\circ}_{\text{assoc}} - \text{Rb}_{(0)}}} \qquad \text{for } \Delta S^{\circ}_{\text{assoc}} = 0, \quad T = T_{\text{S}} \tag{7}$$

As for equine cytochrome *c*, the compensation temperatures T_{S} and T_{H} follow nearly linear temperature dependencies on φ (data not shown). Below the compensation temperature of $T_{\text{H}(\varphi = 0.30)} = 297.9$ K, the interaction is entropically-driven (corresponding to region A), whilst above the compensation temperature of $T_{\text{H}(\varphi = 0.30)} = 300.3$ K the interaction is progressively dominated by enthalpic processes (corresponding to region C). Region B represents the narrow temperature range ($\Delta T = 2.5$ °C) where the transition occurs between enthalpically- and entropically-driven processes for this protein–non-polar ligand interaction, and corresponds to the maximum in the Van't Hoff plot (Fig. 1E) and a minimum in the $\Delta G^{\circ}_{\text{assoc}}$ versus *T* plot (data not shown). Protein–non-polar ligand interactions that are entropically- or enthalpically-driven can be anticipated to result in inherently different patterns of protein stability. Thus, in principle, the maxima or minima in the respective Van't Hoff plots and $\Delta G^{\circ}_{\text{assoc}}$ dependencies on *T* reflect transitions in the conformational status of proteins when heterothermic binding associations occur. Such behaviour has been observed previously for monomeric and dimeric insulins, *fos*/*jun* transcription factors [21] as well as for coiled coil polypeptides derived from the HIV-1_{LA1} envelope glycoprotein gp160 (Jong et al. in preparation).

Eqs. (6) and (7) in particular, in conjunction with entropy–enthalpy compensation (EEC) plots permit the identification of the temperature boundaries defined by T_S and T_H between which EEC occurs as well as the contribution from the enthalpy or entropy change in the interaction without the need to graphically determining these temperatures in Gibbs free energy balance plots (simultaneously plotting ΔH°_{assoc} and $T\Delta S^\circ_{assoc}$ versus T). Since the equilibrium binding constant, K_{assoc}, is a function of ΔS°_{assoc} and ΔH°_{assoc}, changes K_{assoc} can be optimised by appropriate adjustment to these temperature boundaries. Endothermic binding requires large positive entropy changes, not only to compensate for the unfavourable enthalpy change but also provide the necessary binding energy to achieve the observed K_{assoc}. The overall entropy change is the summation of contributions from the solvational entropy change (an energetically favourable term originating from the release of water molecules upon binding), the conformational entropy change (a term originating from the energetically unfavourable loss of conformational degree of freedom from both the ligand and some amino acid residues of the cytochrome *c*s) and the translational entropy change (also an energetically unfavourable term). Since the loss of translational entropy is common for all binding processes, optimisation of the binding of the cytochrome *c*s must focus on maximising the solvational entropy gain (i.e. by increasing the hydrophobicity of the molecule) and by minimising conformational entropy loss (i.e. by increasing the structural rigidity of the molecule). However, as pointed out by Freire and coworkers [25], when the structure of a HIV-1 protease inhibitor was optimised via this strategy (leading to a more rigid, hydrophobic and pre-shaped molecule) the inhibitor had limited capacity to adapt to geometric distortions in the binding site of its receptor due to these mutations. Consequently conformational flexibility is a desirable feature of any protein–ligand interaction, but the thermodynamic consequence of an unfavourable increase in conformational entropy has to be compensated, otherwise low binding affinities are expected to occur. This can be achieved by enthalpically compensating the entropic loss by introducing polar groups into a protein at locations where strong hydrogen bonds, polar van der Waals interactions or salt bridges can be established. Such structural effects (cf. Tables 1–4) arising from the various amino acid substitutions in the different cytochrome *c*s, account for the trends evident in the ECC plots and the Gibbs free energy balance plots for the various cytochrome *c*s investigated in this study.

Table 1
Number of amino acid differences between the five animal cytochrome *c* species, compiled from http://www.embl-heidelberg.de/

	Canine	Chicken	Tuna	Bovine	Equine
Canine	–	10	18	3	6
Chicken	10	–	17	9	11
Tuna	17	16	–	16	18
Bovine	3	9	17	–	3
Equine	6	11	19	3	–

3.3. The heat capacity of the protein–non-polar ligand interaction in acetonitrile–water mixtures

An important thermodynamic parameter associated with protein–ligand interactions is the change in heat capacity, ΔC°_p. In the case of proteins interacting with immobilised non-polar ligands, burial of hydrophobic surfaces of the protein in the non-polar ligand milieu is anticipated to yield large and negative ΔC°_p values [26]. It is widely accepted that under these circumstances, the relative changes in ΔC°_p for the association of a set of closely related protein homologues with the same ligand system will be proportional under the chosen experimental conditions to the accessible surface areas (ASAs) of the proteins, which can be divided into an apolar surface component (with the energetics of the interaction being related to the hydrophobic effect) and a polar surface component (its energetics related to hydrogen bonding) [27,28]. Fig. 3A–E shows that the changes in heat capacity arising from the different cytochrome *c*–*n*-octyl ligands associations are, as expected, large and negative. Moreover, the ΔC°_p differences of these cytochrome *c*s under a specific solvent condition follows the trend expected for these proteins based on their ASAs and the hydrophobicity of the substituted amino acid residues (cf. Tables 1–4). In addition, these results indicate that there is an overall trend of increasing ΔC°_p values for a specific cytochrome *c* measured at a particular solvent condition when the temperature is increased, indicating that the hydrophobic surface areas of the protein and/or ligands accessed by the solvent decreases as T in-

Table 2
Distinguishing amino acids of the five cytochrome *c* species, compiled from http://www.embl-heidelberg.de/, the non depicted amino acid residues are identical

Species	Sequence position number																				
	3	4	9	15	22	28	33	44	46	47	54	58	60	62	88	89	92	95	100	103	104
Canine	Val	Glu	Ile	Ala	Lys	Thr	His	Pro	Phe	Ser	Asn	Thr	Gly	Glu	Thr	Gly	Ala	Ile	Lys	Lys	Glu
Chicken	*Ile*	Glu	Ile	*Ser*	Lys	Thr	His	***Glu***	Phe	Ser	Asn	Thr	Gly	*Asp*	*Lys*	*Ser*	Val	Ile	*Asp*	*Ser*	*Lys*
Tuna	Val	***Ala***	***Thr***	Ala	***Asn***	***Val***	***Trp***	***Glu***	***Tyr***	Ser	***Ser***	***Val***	***Asn***	***Asn***	Lys	Gly	**Gln**	***Val***	***Ser***	***Ser***	
Bovine	Val	Glu	Ile	Ala	Lys	Thr	His	Pro	Phe	Ser	Asn	Thr	Gly	Glu	Lys	Gly	***Glu***	Ile	Lys	***Asn***	Glu
Equine	Val	Glu	Ile	Ala	Lys	Thr	His	Pro	Phe	Thr	Asn	Thr	Lys	Glu	Lys	Thr	Glu	Ile	Lys	Asn	Glu

Amino acids differences between tuna/bovine and chicken/canine cytochrome *c* are depicted in bold and italic. All 21 listed variable amino acid residues are to some extent surface exposed, as found from the corresponding 3D-structures, see Table 4 for additional details.

Table 3
Accessible surface area for two cytochrome *c* species: tuna (Thunnus alalunga from [59]), and equine (Equus caballus from [60])

Cytochrome *c*	PDB file	N_{res}	ΔA_{apolar} (Å^2)	ΔA_{polar} (Å^2)	ΔA_{total} (Å^2)
Tuna	5CYT	103	3602.8	2438.5	6041.3
Equine	1HRC	104	3667.5	2617.0	6284.5

The file identifiers are taken from the Brookhaven Protein Data Bank (PDB) at http://www.rcsb.org/pdb/. N_{res} is the number of amino acids in the sequence. The ASA was calculated using the programs SCRIPT1 at http://www.bork.embl-heidelberg.de/ASC/asc2.html [61,62].

creases. Two processes could account for this behaviour. The first process could arise from a significant re-organisation of the physical structure of the immobilised non-polar ligands due to a phase change. Previously, we have shown [2,7], however, that such phase transitions are not significant contributors to the ΔC_p° variations under the experimental conditions employed in this study. In the second process, the hydrophobic contact area established between the protein and the non-polar ligands could increase as *T* increases due to an unfolding event with greater exposure of previously buried hydrophobic amino acid residues of the protein to the non-polar ligand environment, resulting overall in a smaller effective area of the docked protein–non-polar ligand complex that is accessible to the bulk solvent. This entropy-driven docking of the cytochrome *c*s to the non-polar ligands involving displacement of water molecules from binding sites that previously were filled with a net-work of structured water molecules has parallels involving agonist interaction with β-andrenergic [29] and A_1 adenosine [30] receptors, where displacement of structured water from the 'receptor' binding site and associated conformational re-organisation accounts for the observed larger increase in entropy for agonists. Thus, the differences evident in the interactive behaviour of these proteins as the temperature was increased at a fixed φ-value can be attributed to changes in the extent and nature of the surface exposed residues of the protein as a consequence of conformational changes. Moreover, this conclusion is also consistent with previous studies with G-protein coupled receptors and ligand-gated ion channel receptors imbedded in non-polar environments indicating that solvent effects might similarly be responsible for the in vitro thermodynamic discrimination of their binding behaviour with agonists and antagonists. It is of interest to note that the changes in the heat capacity over the temperature range from 278 K and 338 K for equine cytochrome *c* (8.3 J mol^{-1} K^{-1} per residue) on binding to the *n*-octyl ligands are relatively small and comparable to those observed under similar conditions for 20-mer α-helical polypeptides, like the HIV-1 gp120 CD4 binding site peptide analogues with a corresponding ΔC_p° of ca. 7.6 J mol^{-1} K^{-1} per residue (Jong et al., in preparation) or small peptides with limited secondary structure such as the 7-mer thrombin receptor agonist peptides with a corresponding ΔC_p° of ca. 9.3 J mol^{-1} K^{-1} per residue [31]. Furthermore, the incremental change in heat capacity $\Delta\Delta C_p^\circ$ for the protein–ligand interaction is related to the compactness of the protein and corresponds to its heat sensitivity at a particular solvent condition. The compactness of the protein over a defined temperature range can be related to the extent of temperature-dependent hydrophobic stabilisation of the protein core. For the cytochrome *c*s, this compactness is known to be high because of the stabilising effect of the heme group and the presence of the well established secondary structural elements, i.e. α-helices. The $\Delta\Delta C_p^\circ$ values obtained from this study allow a ranking of the different cytochrome *c* species in terms of their relative stability and compactness at $\varphi = 0.31$ (and a similar ranking can be made for the other solvent compositions) in the presence of the non-polar ligand from the least structurally compact cytochrome *c* to the most compact species: canine ($\Delta\Delta C_p^\circ = 0.82$ kJ mol^{-1} K^{-1}) > chicken ($\Delta\Delta C_p^\circ = 0.78$ kJ mol^{-1} K^{-1}) > bovine ($\Delta\Delta C_p^\circ = 0.72$ kJ mol^{-1} K^{-1}) > tuna ($\Delta\Delta C_p^\circ = 0.64$ kJ mol^{-1} K^{-1}) ≈ equine ($\Delta\Delta C_p^\circ = 0.63$ kJ mol^{-1} K^{-1}). These findings suggest that all of the cytochrome *c*s remain relatively compact during the ligand interactions under the present experimental conditions and do not become fully denatured at the higher temperatures, corroborating other spectroscopic studies [32,33]. In contrast, much larger changes in heat capacity have been observed for the unfolding of insulin in the presence of immobilised non-polar ligands (Boysen et al., in preparation) or the unfolding of the transcription factor c-*jun* [21], both of which shows significant increases in the hydrophobic contact area between protein and the non-polar ligand with increasing temperature.

Table 4
Accessible surface area for each specific amino acids from equine cytochrome *c* calculated from the 1HRC [60] file identifier taken from the Brookhaven Protein Data Bank (PDB) at http://www.rcsb.org/pdb/ [63] utilizing the SCRIPT1 program at http://www.bork.embl-heidelberg.de/ASC/asc2.htm [61,62]

Amino acid	No. of residues in cytochrome *c*	ASA (Å^2)	% Contribution to total surface area
Ala	6	208	3.3
Arg	2	81	1.3
Asn	5	303.8	4.8
Asp	3	166.2	2.6
Cys	2	58.8	0.9
Gln	3	372.8	5.9
Glu	9	877.3	14.0
Gly	12	439.3	7.0
His	3	125.4	2.0
Ile	6	224.9	3.6
Leu	6	65	1.0
Lys	19	2170	34.5
Met	2	73.1	1.2
Phe	4	143.6	2.3
Pro	4	223.2	3.6
Ser	0		0.0
Thr	10	421.5	6.7
Trp	1	13.5	0.2
Tyr	4	96.4	1.5
Val	3	147.6	2.3

3.4. Circular dichroism spectroscopy of the proteins in free solution

Recent CD spectroscopic studies of the globular proteins such as cytochrome *c* in free solution have emphasized the biological importance of non-native conformations. It was shown, for example, that the membrane-bound form of cytochrome *c* has apoptotic activity, suggesting that this conformation, which lacks many features of the free solution tertiary structure but retains a highly helical content, was involved in caspase activation [34]. These observations on the folded status of cytochrome *c* are relevant to the kinetic processes that underscore the current experimental observations. Thus, an important question relates to whether the cytochrome *c*s undergo significant unfolding in the bulk solvent environment prior to binding to the non-polar ligands. These considerations can be addressed, on the one hand, from the framework model of protein folding, which assumes that the formation of each secondary structure element precedes the formation of a tertiary structure [35]. The hydrophobic collapse model, on the other hand, assumes initial condensation of hydrophobic elements that result in compact states without secondary structure [36]. The folding mechanism for eukaryotic cytochrome *c*s remained somewhat controversial and the generalisation of the findings to other proteins has often been questioned due to the presence of the large prosthetic group. Advances in time-resolved CD spectroscopy have resulted in experimental evidence favouring the hydrophobic collapse model for the folding of cytochrome *c*. Here, the hydrophobic collapse of the polypeptide chain may be attributed to the heme group, which is covalently attached to Cys^{14} and Cys^{17}, coordinated via iron to His^{18} and Met^{80}, which act as a hydrophobic nucleation core. The folding/unfolding of cytochrome *c* can then be described by the sequential mechanism U ↔ I ↔ II ↔ N [37] with the characteristics of each of the states, the unfolded, the intermediate states I and II (the latter known as molten globule-like state) and the native state characterized by fluorescence- [38], CD- [32,39,40] and NMR spectroscopy [41]. The successful mapping of the cytochrome *c* from *Saccharomyces cerevisiae* iso-1 energy landscape by fluorescence energy transfer kinetics [42,43] revealed a complex folding funnel. Recently, a consensus folding mechanism for the cytochrome *c* family was proposed, in spite of the large differences in physico-chemical properties and thermodynamic stabilities [44]. According to this Chevron plot based model, the folding mechanism of the cytochrome *c* family can be described by a kinetic three state on-path model U ↔ I ↔ N, if the high energy state reflecting the native penta-coordinated species is ignored. Interestingly, recently published native state hydrogen-deuterium exchange experiments with cytochrome *c* have led to the postulation of five cooperative folding–unfolding units for this protein, termed foldons [45]. These experiments were performed with the rationale that thermodynamic principles require that a protein is continually unfolding and refolding even under native conditions, albeit at very low levels.

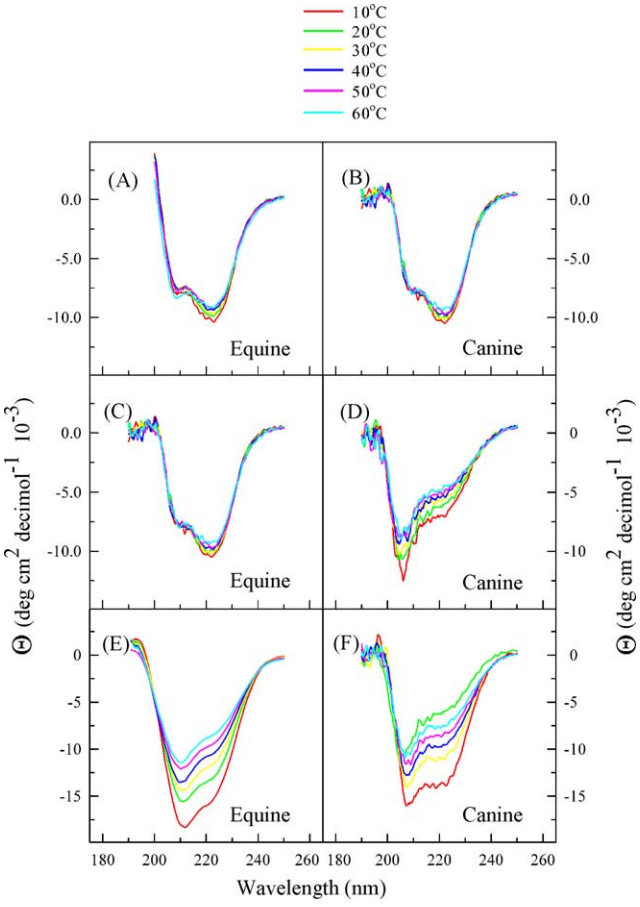

Fig. 5. Illustrative example of the CD spectra of cytochrome *c* from different species, over the temperature range from 10 °C to 60 °C of equine (A) and canine (B) in 10 mM phosphate buffer, pH 7.0 (B), of equine (C) and canine (D) in 30% (v/v) acetonitrile in water, 0.09% TFA corresponding to a φ value of 0.30 and of equine (E) and canine (F) in 60% (v/v) methanol in water, 0.09% TFA corresponding to a φ value of 0.60.

In this process, all possible high-energy intermediate states of the protein are occupied according their Boltzmann equilibrium factor, whereby all molecules continually cycle to through all of these states. Changes in hydrogen exchange rates are observed, when proteins transiently visit their higher energy states, characterised by deprotection reactions (hydrogen bond breaking) of in the native state protected hydrogens.

Thus, Fig. 5A shows the CD spectrum of equine cytochrome *c* over the temperature range from 283 K to 333 K measured in 10 mM sodium phosphate buffer, pH 7.0. Similar results were obtained for canine cytochrome *c*, depicted in Fig. 5B. These findings are in very good agreement with published data for equine cytochrome *c* [39,46] characterized by a double minimum of equal depth, yielding 33% α-helix, 15% of β-strand, and 52% of random structure at 293 K, where the protein has the maximum helicity under this buffer conditions (cf. Table 5). The decrease in helicity when the temperature was decreased to 283 K was 1% and as the temperature was increased to 333 K the helicity change was 2%. These values can be compared to the estimated secondary structure content from free solution NMR spectroscopy measurements, which

yield values for equine cytochrome *c* of 35.6% α-helix, 3.8% of β-strand, 26.8% of β turn and 31.7% of random structure [47]. The relative changes in the secondary structure contents for the different cytochrome *c*s in response to variations in the experimental conditions thus give valuable insights in the folding status of the protein. For example, under the solvent conditions employed in this study at acidic pH, the secondary structure of the acetonitrile-induced conformational state of equine cytochrome *c* remained relatively high, as shown in Fig. 5C, namely of 65% α-helix, 5% β-strand and turn, and 30% random coil structure at 293 K, indicating a structure of increased helicity but distinctly different from the native state. As the temperature was increased to 333 K, the helicity of this solvent-induced conformational state of equine cytochrome *c* continuously decreased to 41%. Under the acidic conditions employed, due to the protonation of His^{33}, misligation of this amino acid residue (instead of ligation of Met^{80}) with the coordination sphere of the iron ion can be excluded from any involvement in the generation or stabilisation of the hydrophobic nucleation core [48,49] of this solvent-induced conformational intermediate of equine cytochrome *c*.

The shape of the CD spectra of the cytochrome *c*s was characterized by a double minimum with a pronounced absolute minimum at 210 nm. The spectra are similar to the spectra of the highly helical alcohol denatured state of cytochrome *c* as described by Konno [39] and to the spectra of the cytochrome *c* intermediate state II described by Akiyama [37], which displays a significant proportion of α-helices. If the data from the time resolved CD spectra of cytochrome *c*s in the range from 400 μs to 6 ms are considered [37], it becomes evident that the relative depth of the minima are continuously shifted during the folding of the protein, whereby in the early stages of folding the minimum at 208 nm is the most pronounced, but with the development of the native state of cytochrome *c* the minimum at 222 nm becomes more dominant. Interestingly, the spectrum shown in Fig. 5C is also similar to the spectrum of cytochrome *c* bound to L-PG micelles and is fundamentally different to the spectrum of the acid denatured state avocet measured in 10 mM HCl at pH 2.0 [46]. The results further emphasise that acetonitrile as a cosolvent in the presence of low concentrations of trifluoroacetic acid has α-helix stabilizing properties as result of its poor hydrogen bonding properties. In contrast, low concentrations of trifluoroacetic acid in water alone destabilises the secondary structure of the different cytochrome *c*s [50] since the balance between stabilizing hydrophobic interactions and disruptive charge-charge repulsion between positively charged groups is shifted. In summary, when compared to the available literature data, the cytochrome *c*s over the temperature range from 283 K to 333 K (in 30% acetonitrile, 0.1% TFA in water) maintain conformational structures that are relatively compact, which can be best described as the intermediate state II, prior to binding to the non-polar ligands. In contrast, to this, Fig. 5E shows the CD spectrum of equine cytochrome *c* over the temperature

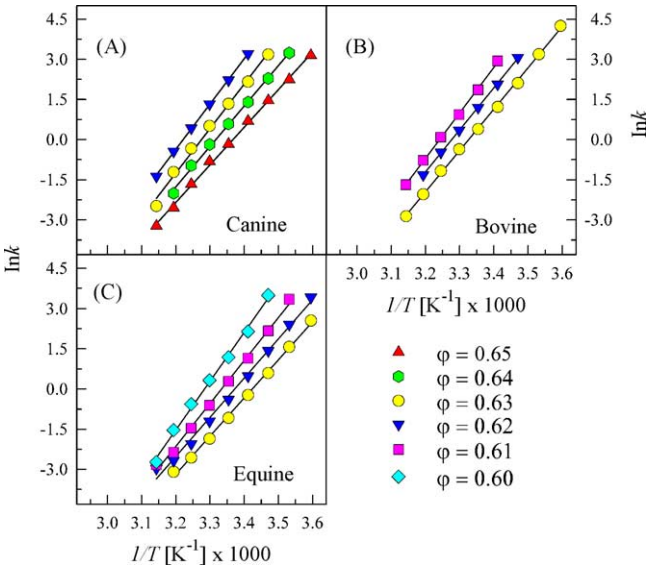

Fig. 6. Van't Hoff plots of the logarithmic binding variable ln *k* vs. 1/*T* for canine (A), bovine (B) and equine (C) cytochrome *c* at different volume fractions, *φ*, of methanol in the water–organic solvent mixture.

range from 283% to in 60% methanol 0.1% TFA in water. Here, a significant decrease in helicty is observed when the temperature is increasing, indicating a temperature induce unfolding.

3.5. Cytochrome c–ligand interaction in the presence of methanol as cosolvent

The Van't Hoff plots (ln *k* versus 1/*T*) for equine, bovine and canine cytochrome *c* using the water–methanol system were in all cases linear and could be fitted with high correlation to a first order dependency (Fig. 6A–C) with $\Delta H^{\circ}_{\text{assoc}}$, $\Delta S^{\circ}_{\text{assoc}}$, and ΔC°_{p} calculated as described above.

3.6. Gibbs free energy balance of cytochrome c ligand–interaction in the water–methanol solvent systems

In contrast to the interaction behaviour of cytochrome with the non-polar ligands in water–acetonitrile systems, the interaction of bovine and human cytochrome *c* with the immobilised *n*-octyl ligands in the water–methanol system is associated with linear and constant dependencies of enthalpy and entropy on *T* as (data not shown).

3.7. The entropy–enthalpy compensation of the protein–non-polar ligand interaction in methanol-water mixtures

When $T\Delta S^{\circ}_{\text{assoc}}$ is plotted against $\Delta H^{\circ}_{\text{assoc}}$, then the specific influences of the solvents become apparent (data not shown). Whilst for cytochrome *c*–ligand interaction in water–acetonitrile the interaction is entropy or/and enthalpy driven depending on the temperature, the cytochrome-ligand

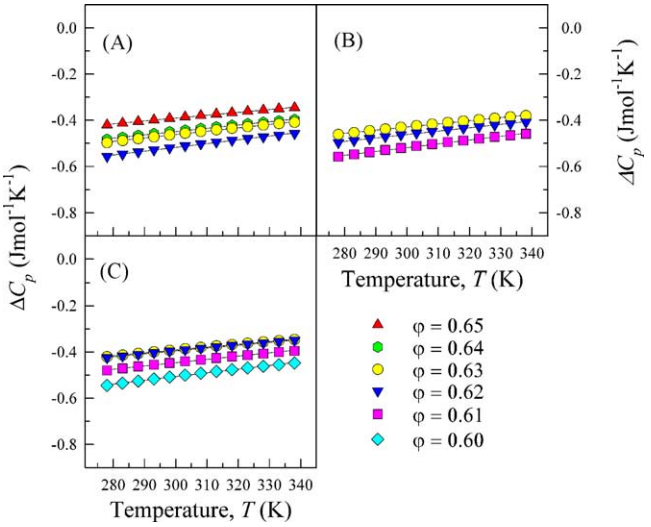

Fig. 7. Plots of the change in heat capacity, ΔC_p°, vs. T for canine (A), bovine (B) and equine (C) cytochrome *c* at different volume fractions, φ, of methanol in the water–organic solvent mixture.

interaction in water–methanol is exclusively enthalpy driven at all temperatures.

3.8. The heat capacity of the protein–non-polar ligand interaction in methanol-water mixtures

The change in the heat capacity, ΔC_p°, for the cytochrome *c*s in methanol-water was found to be constant over the whole temperature range. Although the change in heat capacity of the cytochrome *c*–*n*-octyl ligand interaction in the methanol–water-system was negative for most temperatures, as seen from Fig. 7A–C, the change in heat capacity over the entire temperature range is smaller by a factor of approximately 10-fold compared to the changes observed for the water–acetonitrile–water system [canine $(\Delta\Delta C_p^\circ = 0.08\,\mathrm{J\,mol^{-1}\,K^{-1}}) \approx$ bovine $(\Delta\Delta C_p^\circ = 0.08\,\mathrm{J\,mol^{-1}\,K^{-1}}) \approx$ equine $(\Delta\Delta C_p^\circ = 0.08\,\mathrm{J\,mol^{-1}\,K^{-1}})$].

In order to interpret the temperature dependence of the heat capacity, ΔC_p° in the cytochrome *c*–ligand interaction with water–methanol in conjunction with the results from the free solution structure as obtained with CD spectroscopy, it is necessary to consider the factors from which the change in heat capacity is normally derived. In the past, large heat capacity effects have been associated with hydrophobic interactions [51] in which the magnitude was correlated with the change in solvent-accessible surface areas. At the molecular level, the decreased heat capacity upon protein folding or protein–protein interaction (and the accompanying release of thermal energy) is usually pictured as a direct consequence of the reorganisation of the liquid-water lattice around non-polar groups of the protein.

The absence of an appreciable ΔC_p° value in the cytochrome *c*–ligand interaction in water–methanol can be seen as evidence that there are no temperature dependent structural changes, or alternatively no change in the volume of the protein. The retention of cytochrome in RP-HPLC in water–methanol was reduced when the temperature was increased. In water–methanol the cytochromes behave thermodynamically similar to a rigid, low molecular weight compound, which cannot change its accessible surface area). In the absence of solvent ordering contribution of hydration ΔH^{Hyd} for methanol, the Lifshitz–van der Waals component ΔH^{vdW} of the hydrophobic effect for the interactive cytochrome *c*–ligand process ($\Delta H^{\mathrm{HPH}} = \Delta H^{\mathrm{vdW}} + \Delta H^{\mathrm{Hyd}}$) prevails with $\Delta H^{\mathrm{HPH}} \approx \Delta H^{\mathrm{vdW}}$. The cytochrome *c* stays folded, the proportionality between ΔC_p° and ASA is valid, with the low ΔC_p° value reflecting the size the of the hydrophobic interaction patch.

For ubiquitin, the disappearance of ΔC_p° is a function of the methanol concentration [52]. This could be related to the composition of water–methanol mixtures. In binary methanol water mixtures, a ternary system composed of water, water-associated methanol and methanol exists. Herein free methanol is the chromatographically active species [20]. At a solvent mixtures from 0% to 30% methanol (v/v) the mixtures contains very little free methanol, at 80–100% methanol (v/v) the mixtures contain very little free water. Recently similar investigations have been extended to acetonitrile, whereby the spectra of a water-solvated solute, cosolvent-solvated solute and the water-cosolvent-complex-solvated solute revealed the concentration profile of the individual components for acetonitrile and methanol, respectively [53]. In this study, the disappearance of the heat capacity signature seems to coincide with a high free methanol content.

Recently, the wider applicability of the correlation of heat capacity and the accessible surface area has been questioned. It was shown that the heat capacity can arise generally in order-disorder transitions in systems with hydrogen-bonded networks. Herein the thermodynamics of protein folding or protein–protein interaction were described as a mixture of polar and non-polar effects [54]. The wider implications of this approach, at least at first site, are not clear, in particular in the light of the emerging insights into the solvatochromic parameters of dipolarity/polarizability, π^*, and the hydrogen bonding activity (α) of methanol and acetonitrile [53]. In view of the lack of understanding of their temperature dependence, one might question the causal dependency for the heat capacity change/ASA correlation for methanol as a cosolvent. It becomes apparent, that the dipolarity/polarizability values, π^*, (water: 1.09, methanol: 0.59, acetonitrile 0.71, [55]) and the α-values (water: 1.05, methanol: 1.0, acetonitrile 0.37 [56]) for the pure solvents should be substituted by summated effects of the respective values of solvent alone, water alone and solvent–water complex at a particular solvent composition [53]. One could argue that hydrogen bonding characteristics of water–methanol in regard to its temperature characteristics, and consequently, if one follows the alternative view of heat capacity, the absolute heat capacity of the water–methanol solvent is altered in a way so that there are no heat capacity differences of the folded or unfolded pro-

Table 5
Amino acid sequence from equine cytochrome *c*

GDVEKGKKIF	VQKCAQCHTV	EKGGKHKTGP	NLHGLFGRKT	GQAPGFTYTD
HHHHHHHH	HHHTTTT	STT SS	TTTTTSBS	S TT H
ANKNKGITWK	EETLMEYLEN	PKKYIPGTKM	IFAGIKKKTE	REDLIAYLKK
HHHH B S	HHHHHHHTTT	HHHHSTT S	SHHH	HHHHHHHHHH
ATNE				
HS				

The sequence is depicted in the single letter code. Secondary structure was calculated according to the method of Kabsch and Sander [64]. The assignments are: H: helix; B: residue in isolated β-bridge; E: extended β-strand; G = 3_{10} helix; I = π-helix; T: hydrogen bonded turn; S: bend.

tein. Consequently, conformational changes for cytochrome *c* in methanol water mixtures in the presence of hydrophobic ligands may occur with no overall net gain or loss of hydrogen bonding. If this is the case one could conclude, that the cytochrome *c* in the methanol system suffers no observable conformational changes in the presence of a hydrophobic ligand. Since the CD spectroscopy data show (Fig. 5C) that cytochrome *c* unfolds in free solution when the temperature is increased, it can be further concluded that the presence of a hydrophobic ligand exerts a stabilising effect on the protein.

4. Conclusions

Our experimental findings, based in particular on the derivation of the heat capacity values and the spectroscopic data suggest that during the adsorption process to the solvated *n*-octyl ligands the cytochrome *c*s resembles compact molecules, which behave like a molten globule folded intermediates with a high content of α-helicity. The extent of α-helicity depends on the temperature employed in the measurements. Utilisation of the 3D data of the cytochrome *c*s together with the finding that these proteins can interact with an orientational preference with immobilised *n*-alkyl ligands [57] insight has previously been gained into the molecular characteristics of the binding domain. However, this approach does neither permit the contribution of individual amino acid residues to be directly deciphered at an atomic level nor permit the contribution of secondary retention effects, i.e. interaction of the ε-amino groups of lysine residues with free silanol groups of the sorbent to be delineated. The involvement of conformational transitions and their consequences in terms of the extent of exposure of formerly buried amino acid residues cannot be deduced a priori by this molecular footprinting approach, despite the fact that the respective amino acids involved in the binding domain, i.e. within the amino acid sequence from residues 56–104, across the different cytochrome *c* species can be identified (Table 2). For example, as apparent from the present study, equine and bovine cytochrome *c* differ only in three residues (Table 1), two of which fall within the protein–ligand contact area, namely residues Xaa^{60} and Xaa^{89} (Table 2). If the contribution of individual amino acids to the overall accessible surface area is considered (cf. Tables 3 and 4) it is apparent that Lys residues represents ca. 34.5% of the ASA of the native cytochrome *c*s in their bulk solution state. The presence of Lys^{60}, $Lys^{72–73}$, Lys^{79}, $Lys^{99–100}$ in the binding domain(s) of the cytochrome *c*s in association with *n*-octyl ligands has been established previously [57] from the enzymatic digest footprint studies with these residues becoming inaccessible to trypsin when the cytochrome *c*s were bound to these ligands. The overall small differences in k' values for equine cytochrome in comparison with bovine cytochrome *c* is consistent with the substitution of Lys^{60} in the equine cytochrome *c* by Gly^{60} in the bovine cytochrome *c*. As apparent from a comparison of the amino acid substitution patterns for the various cytochrome *c*s (Tables 1 and 2) other amino residues i.e. Thr^{89} in equine cytochrome *c*, in addition to these clustered Lys residues, will make significant contributions to hydrophobic interaction with the non-polar ligands. In equine cytochrome *c*, the Thr^{89}, with an ASA of 87.8 $Å^2$, is highly surface exposed as evident from the 3D-structure. Paradoxically, replacement of Thr^{89} in equine cytochrome *c* with the much smaller Gly^{89} in the bovine cytochrome *c* appears to reinforce the hydrophobic interaction of the cytochrome *c* binding domain with the *n*-octyl ligands as the magnitude of the *k* values suggest, since it is likely, that Thr^{89}, due to its size and polarity sterically hinders the interaction of the non-polar ligands with the much larger hydrophobic surface in equine cytochrome *c*. Once docked, these same residues are likely to contribute in a similar manner to the binding energy, even when the α-helices in the binding domain have partially unwound under the influence of increasing temperature.

In water–acetonitrile, the cytochrome *c*–ligand interaction is enthalpy or entropy driven, or both, depending on the temperature. The heat capacity/temperature dependency in conjunction with the Gibbs free energy balance was interpreted as an unfolding process of the protein with the two states, the folded and the unfolded, characterized by a set of compensation points. The hydration effects and the Lifshitz–van der Waals interactions contribute to the hydrophobic interactions between cytochrome *c* and ligand. With the described thermometric HPLC procedure, using water–acetonitrile solvents, the thermodynamic stability of the hydrophobic core of the cytochrome *c* species can be measured and ranked.

In contrast, in water–methanol the cytochrome *c*–ligand interaction is entirely enthalpic. The heat capacity values

are close to zero and lack pronounced temperature dependence. This could be seen as evidence that cytochrome *c* was only in one conformational state, which is not necessarily the native and that the conformation of cytochrome *c* is possible stabilised by the presence of a non-polar ligand. On the other hand it could be argued that the heat capacity/ASA correlation is not applicable for the water–methanol solvent mixtures. Rather, a nearly constant heat capacity could be interpreted in the sense that there is no net gain or loss of hydrogen bonds in the ternary system (ligand, solute and solvent) as the temperature is varied. Consequently occurring structural changes could not be monitored. Since the self-hydrogen bonding of methanol ($\gamma^{AB} = 4.3\,mJ/m^2$) in relation to water ($\gamma^{AB} = 51\,mJ/m^2$) is drastically reduced (organic solvents must posses less self-hydrogen bonding then water in order to achieve elution in RP-HPLC) [58], its is believed, that under the methanol concentrations employed, only the Lifshitz–van der Waals effect contributes to the cytochrome *c*–ligand interaction and is too weak to promote unfolding of cytochrome *c* in the presence of an the conformation stabilising ligand. In fact, under the conditions employed, the cytochrome *c* dissociated in the presence of the ligand before it could unfold at high temperatures. With the described thermometric HPLC procedure, using water–acetonitrile mixtures, the differences of proteins with respect to their protein surface–ligand interaction can be measured and ranked according the size of the interacting hydrophobic surface.

In summary, the approach presented in this paper provides an avenue to evaluate the interactive and conformational behaviour of polypeptides and proteins in the presence of solvated non-polar ligands, thus permitting improved understanding of the underlying molecular properties that link the thermodynamic and extra-thermodynamic relationships, rather than relying on empirical treatments as have been commonly employed in the past. In subsequent papers we will report the application of this approach in the determination of thermodynamic parameters of genetically engineered as well as naturally occurring proteins in different types of water–organic solvent mixtures or other systems and in particular the assessment of the thermostability of peptides and proteins in non-polar environments in the context of the mutational adaptation of these biomolecules, not only in terms of their effect on specific biochemical functions, but also with regard to their impact on recovery of bioactivity in biotechnological purification processes per se.

Nomenclature

ΔA_{apolar} apolar accessible surface area
ΔA_{polar} polar accessible surface area
ΔA_{total} total accessible surface area
$b_{(0)}$, $b_{(1)}$, $b_{(2)}$, $b_{(3)}$, ... coefficients for the polynomial dependency on $\ln k$ on $1/T$
c_I mole fraction of displacing solvent
ΔC_p° change in the heat capacity for the association of the polypeptide P_i with the non-polar ligates
ΔG_{assoc}° change in Gibbs free energy due to the association of the polypeptide P_i with the non-polar ligates
ΔG_{unfold}° change in Gibbs free energy upon unfolding (denaturation)
ΔH_{assoc}° change in the enthalpy due to the association of the polypeptide, P_i, with the non-polar ligates
ΔH_{unfold}° change in the enthalpy due to unfolding of the polypeptide, P_i, with the non-polar ligates
I intermediate state in three state on-path model $U \leftrightarrow I \leftrightarrow N$
k retention factor and unitless variable ($=n_S/n_M \times V_S \times V_M = K_{assoc} \times \Phi$)
$\ln k$ logarithm of the retention factor, k
$\ln k_0$ value of $\ln k'$ when $c_i \rightarrow 0$, or $\varphi \rightarrow 0$
K temperature (K)
K_{assoc} equilibrium association constant
n_M number of moles of the protein in free solution
n_S number of moles of the protein that exists in bound states
N native state in three state on-path model $U \leftrightarrow I \leftrightarrow N$
N_{res} number of amino acid residues in a polypeptide
N_S moles of protein bound to *n*-polar sorbent
$[P]_{bound}$ the concentrations of the protein in the bound state
$[P]_{free}$ the concentrations of the protein in the free state
r^2 correlation coefficient
R gas constant
ΔS_{assoc}° change in the entropy due to the association of the polypeptide P_i with the non-polar ligates
ΔS_{unfold}° change in the entropy due unfolding of the polypeptide P_i with the non-polar ligates
T temperature (K)
T_{COLD} temperature at which $\Delta H_{assoc}^\circ = T\Delta S_{assoc}^\circ$, with $T_{COLD} < T_{HOT}$
T_{COMP} slope of the entropy–enthalpy compensation plots
T_H temperature at which $\Delta H_{assoc}^\circ \rightarrow 0$
T_{HOT} temperature at which $\Delta H_{assoc}^\circ = T\Delta S_{assoc}^\circ$, with $T_{HOT} > T_{COLD}$
T_S temperature at which $T\Delta S_{assoc}^\circ \rightarrow 0$
U unfolded state in three state on-path model $U \leftrightarrow I \leftrightarrow N$
V_M volume of the bulk liquid in the system
V_S volume of the immobilised ligands on an inert solid support material
V_T total column volume

Greek letters
α hydrogen bonding activity
γ^{AB} self-hydrogen bonding
Θ ellipticity
π^* dipolarity/polarizability value
Φ phase ratio of the system
φ volume fraction of organic solvent in binary water–solvent mixture

Acknowledgement

These investigations were supported by the Australian Research Council.

References

[1] M.T.W. Hearn, in: S. Ahuja (Ed.), Handbook of Bioseparations, 2000, p. 71.
[2] M.T.W. Hearn, in: M.A. Vijayalakshmi (Ed.), Theory and Practice of Biochromatography, Harwood, Switzerland, 2001.
[3] M.T.W. Hearn, Chromatogr. Sci. Ser. 87 (2002) 99.
[4] E.L. Kovrigin, S.A. Potekhin, Biophys. Chem. 83 (2000) 45.
[5] A.W. Purcell, G.L. Zhao, M.I. Aguilar, M.T.W. Hearn, J. Chromatogr. A 852 (1999) 43.
[6] R.I. Boysen, M.T.W. Hearn, in: J.E. Coligan, B.M. Dunn, H.L. Ploegh, D.W. Speicher, P.T. Wingfield (Eds.), Current Protocols in Protein Science, Wiley, New York, 2001, p. 1.
[7] R.I. Boysen, Y. Wang, H.H. Keah, M.T.W. Hearn, Biophys. Chem. 77 (1999) 79.
[8] M.T.W. Hearn, G.L. Zhao, Anal. Chem. 71 (1999) 4874.
[9] F. Eisenhaber, P. Argos, Protein Eng. 9 (1996) 1121.
[10] T.E. Creighton, Proteins: Structures and Molecular properties, W.H. Freemann & Co., New York, 1993, p. 227.
[11] P.G. Squire, M.E. Himmel, Arch. Biochem. Biophys. 196 (1979) 165.
[12] V.Z. Spassov, A.D. Karshikoff, R. Ladenstein, Protein Sci. 4 (1995) 1516.
[13] D. Eisenberg, R.M. Weiss, T.C. Terwilliger, Proc. Natl. Acad. Sci. U.S.A. 81 (1984) 140.
[14] M.A. Andrade, P. Chacón, J.J. Merelo, F. Morán, Protein Eng. 6 (1993) 383.
[15] J.J. Merelo, M.A. Andrade, A. Prieto, F. Morán, Neurocomputing 6 (1994) 443.
[16] M.T.W. Hearn, R.I. Boysen, Y. Wang, S. Muraledaram, in: Y. Shimonishi (Ed.), Peptide Science—Present and Future, Kluwer, Dordrecht, Boston, London, 1999, p. 240.
[17] K.P. Murphy, Biophys. Chem. 51 (1994) 311.
[18] L.A. Cole, J.G. Dorsey, K.A. Dill, Anal. Chem. 64 (1992) 1324.
[19] R.L. Hansen, J.M. Harris, Anal. Chem. 67 (1995) 492.
[20] E.D. Katz, C.H. Lochmuller, R.P.W. Scott, Anal. Chem. 61 (1989) 349.
[21] R.I. Boysen, A.J.O. Jong, J.A. Wilce, G.F. King, M.T.W. Hearn, J. Biol. Chem. 277 (2002) 23.
[22] A. Cooper, Curr. Opin. Chem. Biol. 3 (1999) 557.
[23] J.D. Dunitz, Chem. Biol. 2 (1995) 709.
[24] E. Gallicchio, M.M. Kubo, R.M. Levy, J. Phys. Chem. B 104 (2000) 6271.
[25] A. Velazquez-Campoy, M.J. Todd, E. Freire, Biochemistry 39 (2000) 2201.
[26] P.D. Ross, M.V. Rekharsky, Biophys. J. 71 (1996) 2144.
[27] K.P. Murphy, Med. Res. Rev. 19 (1999) 333.
[28] K.P. Murphy, S.J. Gill, J. Mol. Biol. 222 (1991) 699.
[29] G.A. Weiland, K.P. Minneman, P.B. Molinoff, Nature 281 (1979) 114.
[30] P.A. Borea, K. Varani, L. Guerra, P. Gilli, G. Gilli, Mol. Neuropharmacol. 2 (1992) 273.
[31] R.I. Boysen, A.J.O. Jong, M.T.W. Hearn, Biophys. J. 82 (2002) 2279.
[32] Y. Hagihara, M. Oobatake, Y. Goto, Protein Sci. 3 (1994) 1418.
[33] M. Panda, M.G. Benavides-Garcia, M.M. Pierce, B.T. Nall, Protein Sci. 9 (2000) 536.
[34] R. Jemmerson, J. Liu, D. Hausauer, K.P. Lam, A. Mondino, R.D. Nelson, Biochemistry 38 (1999) 3599.
[35] P.S. Kim, R.L. Baldwin, Annu. Rev. Biochem. 51 (1982) 459.
[36] K.A. Dill, Biochemistry 24 (1985) 1501.
[37] S. Akiyama, S. Takahashi, K. Ishimori, I. Morishima, Nat. Struct. Biol. 7 (2000) 514.
[38] G.A. Elove, A.F. Chaffotte, H. Roder, M.E. Goldberg, Biochemistry 31 (1992) 6876.
[39] T. Konno, J. Iwashita, K. Nagayama, Protein Sci. 9 (2000) 564.
[40] Y. Kuroda, S. Kidokoro, A. Wada, J. Mol. Biol. 223 (1992) 1139.
[41] B.S. Russell, R. Melenkivitz, K.L. Bren, Proc. Natl. Acad. Sci. U.S.A. 97 (2000) 8312.
[42] J.G. Lyubovitsky, H.B. Gray, J.R. Winkler, J. Am. Chem. Soc. 124 (2002) 5481.
[43] J.G. Lyubovitsky, H.B. Gray, J.R. Winkler, J. Am. Chem. Soc. 124 (2002) 14840.
[44] C. Travaglini-Allocatelli, S. Gianni, M. Brunori, Trends Biochem. Sci. 29 (2004) 535.
[45] H. Maity, M. Maity, S. Walter Englander, J. Mol. Biol. 343 (2004) 223.
[46] N. Sanghera, T.J.T. Pinheiro, Protein Sci. 9 (2000) 1194.
[47] A.D. Robertson, K.P. Murphy, Chem. Rev. 97 (1997) 1251.
[48] S.-R. Yeh, S. Han, D.L. Rousseau, Acc. Chem. Res. 31 (1998) 727.
[49] S.-R. Yeh, S. Takahashi, B. Fan, D.L. Rousseau, Nat. Struct. Biol. 4 (1997) 51.
[50] A. Ahmad, K.P. Madhusudanan, V. Bhakuni, Biochim, Biophys, Acta Protein Struct. Mol. Enzymol. 1480 (2000) 211.
[51] K.A. Dill, Biochemistry 29 (1990) 7133.
[52] D.N. Woolfson, A. Cooper, M.M. Harding, D.H. Williams, P.A. Evans, J. Mol. Biol. 229 (1993) 502.
[53] S. Nigam, A. De Juan, R.J. Stubbs, S.C. Rutan, Anal. Chem. 72 (2000) 1956.
[54] A. Cooper, Biophys. Chem. 85 (2000) 25.
[55] M.J. Kamlet, J.L.M. Abboud, M.H. Abraham, R.W. Taft, J. Org. Chem. 48 (1983) 2877.
[56] R.W. Taft, M.J. Kamlet, J. Am. Chem. Soc. 98 (1976) 2886.
[57] M.I. Aguilar, D.J. Clayton, P. Holt, V. Kronina, R.I. Boysen, A.W. Purcell, M.T.W. Hearn, Anal. Chem. 70 (1998) 5010.
[58] C.J. van Oss, Interfacial Forces in Aqueous Media, Marcel Dekker, New York, Basel, Hong Kong, 1994.
[59] T. Takano, R.E. Dickerson, Proc. Natl. Acad. Sci. U.S.A. 77 (1980) 6371.
[60] G.W. Bushnell, G.V. Louie, G.D. Brayer, J. Mol. Biol. 214 (1990) 585.
[61] F. Eisenhaber, P. Argos, J. Comput. Chem. 14 (1993) 1272.
[62] F. Eisenhaber, P. Lijnzaad, P. Argos, C. Sander, M. Scharf, J. Comput. Chem. 16 (1995) 273.
[63] J.L. Sussman, D.W. Lin, J.S. Jiang, N.O. Manning, J. Prilusky, O. Ritter, E.E. Abola, Acta Crystallogr. 54 (1998) 1078.
[64] W. Kabsch, C. Sander, Biopolymers 22 (1983) 2577.